18TH WORLD CONFERENCE ON EARTHQUAKE ENGINEERING
WCEE2024
MILAN

MILAN, ITALY
30TH JUNE - 5TH JULY 2024

www.wcee2024.it

RESILIENT DESIGN OF BUILDINGS USING SHAPE MEMORY ALLOY CABLE-BASED SELF-CENTERING DEVICES

F. Shi[1], and O.E. Ozbulut[2]

[1] School of Physics and Materials Science, Guangzhou University, Guangzhou, China, shifei@gzhu.edu.cn

[2] Department of Civil and Environmental Engineering, University of Virginia, Charlottesville, VA, USA, ozbulut@virginia.edu

Abstract: *This paper introduces a novel hybrid damper called the Superelastic Friction Damper (SFD) and evaluates its performance through nonlinear time history analyses. The SFD combines the high tensile resistance and excellent self-centering capability of shape memory alloy (SMA) cables with the non-sacrificial energy dissipation provided by a frictional damping mechanism. First, the anchorage system and the mechanical properties of the SMA cables are introduced. Subsequently, the configuration and basic working principle of the SFD are detailed, emphasizing its advantages over existing SMA-based hybrid dampers. Next, the fabrication of a prototype SFD and its experimental testing are discussed. The mechanical response of the damper is investigated under repeated cyclic loading, considering various displacement amplitudes and loading rates. Additionally, a numerical model of a steel frame structure incorporating the SFD is developed and analyzed using nonlinear dynamic analysis in OpenSees. This investigation explores the impact of the SFD on enhancing the seismic performance of the structure. The results reveal that the SFD exhibits stable hysteretic behavior with minimal sensitivity to loading rate. The damper provides an equivalent viscous damping of 12%, accompanied by an impressive 89% recovery of the peak damper displacement. The SFD effectively reduces the seismic response of the steel frame structure under Design Basis Earthquake (DBE) and Maximum Considered Earthquake (MCE) hazard levels, particularly in terms of residual inter-story drift ratio (RIDR).*

1 Introduction

Passive energy dampers, including friction dampers, viscous dampers, and buckling restrained braces (BRBs), play a critical role in earthquake resilience by mitigating building response and damage. While they offer numerous advantages when compared to alternative seismic protection measures, they fall short in addressing permanent or residual drift, a challenge that can lead to the need for extensive repairs or even demolition, resulting in substantial economic losses. Residual drift, the degree to which a building tilts or shifts after enduring a seismic event, holds immense significance as it directly influences the building's post-event functionality and the feasibility of repair efforts (Ramirez and Miranda, 2012).

In recent years, self-centering passive devices have garnered increasing attention due to their remarkable earthquake resilience and the unique capacity to restore a building to its original position with minimal structural damage. Several mechanisms such as pre-tensioned cables, preloaded disc springs, pre-pressed springs have been investigated to enable self-centering. For example, Fang et al. (2021) explored a self-centering solution employing preloaded disc springs in conjunction with friction energy dissipation devices, effectively mimimizing residual drifts. Xu et al. (2016) introduced and tested a self-centering brace that combines pre-pressed springs with a friction energy dissipation device. Li et al. (2021) developed a novel self-centering hybrid damper, combining a viscous damper with pre-compressed friction springs.

Among different self-centering mechanisms currently under investigation, shape memory alloy (SMA) stands out as a promising option due to its remarkable ability to revert to its original shape even after experiencing substantial deformations while also serving as an energy dissipating material (Ozbulut et al., 2011). Numerous researchers have explored developing SMA-based devices, skilfully combining SMA with diverse energy dissipation technologies. For instance, Salehi et al. (2021) introduced an innovative SMA-based multi-ring (SBMR) device that utilizes superelastic SMA rings in tandem with energy dissipating rings. Notably, these SMA-based dampers demonstrate adaptability in terms of load application from multiple directions, rendering them a versatile choice for retrofitting buildings, as they can be seamlessly integrated into a wide array of bracing systems. Issa and Alam (2019) explored a novel piston-based self-centering bracing system wherein NiTi SMA bars are inserted within a sleeve-piston arrangement, endowing the structure with self-centering capabilities. Wang et al. (2020) contributed insights into the mechanical properties and behavior of superelastic SMA angles, offering promise as a prospective self-centering device. Zhang et al. (2020) pioneered the development of a novel device known as the deformation-amplified SMA-friction damper, tailored for reinforced concrete frame structures.

While these SMA-based devices exhibit favourable qualities, many of them currently exist as small-scale prototypes without a clearly defined roadmap for their scale-up and full-scale implementation. This is primarily attributed to the utilization of SMA wires in certain devices, which often results in limited force capacities, or the incorporation of SMA bars that pose machining and anchoring challenges. Recently, the utilization of large-diameter SMA cables has paved the way for the advancement of full-scale SMA-based seismic control devices and bracing systems (Silwal et al. 2015; Shi et al., 2018, 2022, 2023). SMA cables are comprised of numerous individual SMA wires and exhibit a remarkable capacity to withstand high levels of tensile forces, all while preserving the superelastic characteristics inherent to SMA materials.

This paper proposes a hybrid self-centering device, Superelastic Friction Damper (SFD), consisting of high-capacity self-centering SMA cables and energy-dissipating friction dampers. Firstly, a detailed description of SMA cables and their anchoring methods is provided. Subsequently, the configuration, experimental testing, and mechanical properties of the novel SFD are elucidated. Finally, this paper further explores the enhancement of the structural seismic resilience by SFD through numerical simulations.

2 SMA cables and its end anchorage

The SMA cable used in this study is made out of Nickel-Titanium (NiTi) with 56.06% Ni. It is structured with 49 wires, each having a diameter of 0.885 mm, organized in a 7x7 arrangement. Specifically, the SMA cable comprises seven strands, with the outer six strands wound around the core strand in a right-handed helical pattern. Each strand consists of seven wires coiled in a left-handed helical form. The outer diameter of the SMA cable measures 8 mm, and its cross-sectional area is 30.13 mm².

A robust anchorage system is essential for ensuring dependable load transfer and averting premature failures and plays an important role in the advancement and deployment of self-centering systems based on SMA cables. (Shi et al., 2021). The anchorage system employed for SMA cables in this study consists of a barrel, a stop end, a compression screw, and a hexagonal nut. Within this mechanical anchorage system, the stop end serves the crucial function of confining the SMA cables within the anchor barrel. SMA cables are initially placed within the anchor barrel, and subsequently, the stop end is affixed to one end of the cables. Mechanical pressure is then exerted on the stop end to securely fasten the SMA cables. Next, the stop end is advanced through the anchor barrel, and a compression screw is employed to secure the stop end firmly within the barrel. The components and assembly process of SMA end anchorage system are shown in Figure 1.

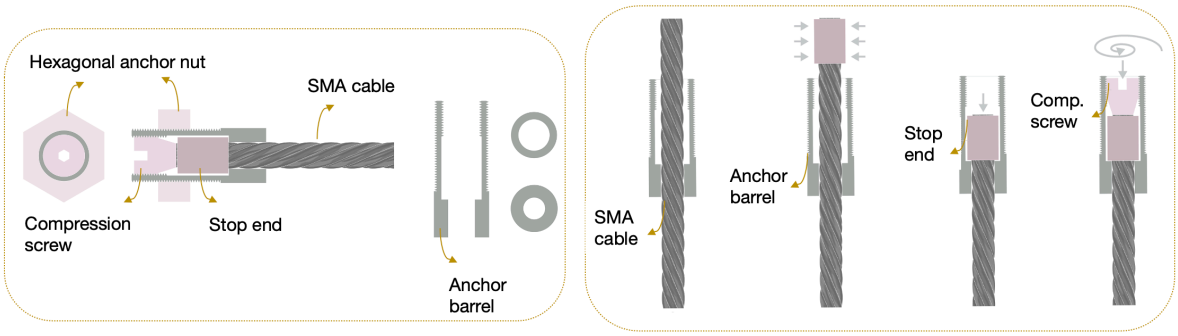

Figure 1. Component of SMA end anchorage system and its assembly

Figure 2 illustrates the tensile response of SMA cables at 6% strain during increasing loading cycles at room temperature. The results show that SMA cables can effectively recover applied strains upon unloading and exhibit excellent superelasticity. However, during cyclic loading, the response curve shifts downward for the initial loading cycles, as depicted in Figure 2(a). Both the forward and reverse phase transformation stress levels of SMA cables decrease with an increasing number of loading cycles. The decrease in forward phase transformation levels is more prominent, resulting in a smaller hysteresis area for higher loading cycles. Nonetheless, this effect diminishes rapidly, and the behavior of the SMA cables largely stabilizes after the first 30 loading cycles. As shown in Figure 2(b), an additional 30 loading cycles have minimal impact on the response of the SMA cables. Therefore, it is suggested to 'train' the SMA cables by subjecting them to cyclic loading before their use in an SMA-based device.

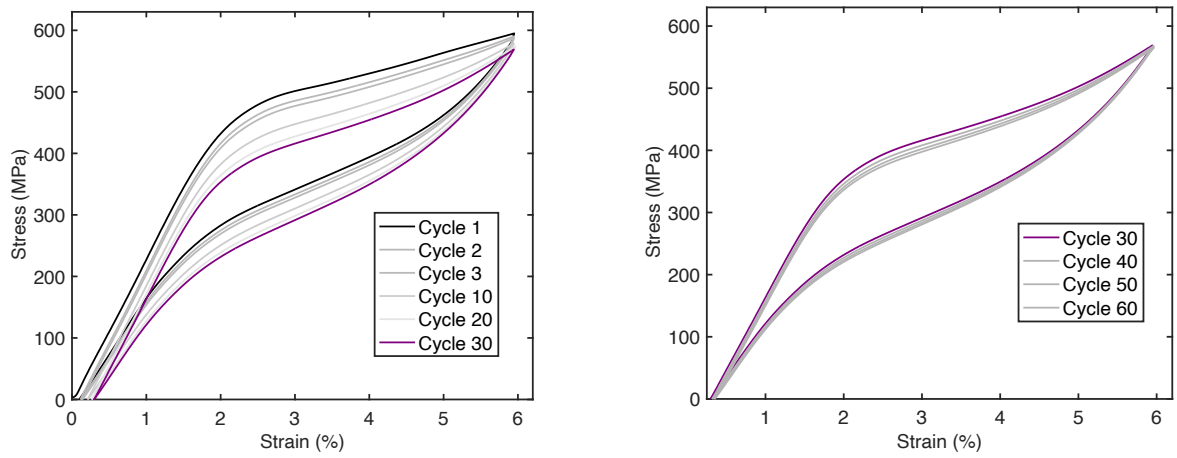

(a) *(b)*

Figure 2. Stress-strain curves of SMAs at 6% strain loading: (a) Cycles 1-30 and (b) cycles 30-60.

It is important to note that SMA cables exhibit the capacity to bear substantial loads even beyond 6% strain. In Figure 3(a), you can observe the behavior of SMA cables within the 6-10% strain range, while Figure 3(b) demonstrates their response within the 10-14% strain amplitudes. When subjected to strains exceeding 7%, SMA cables exhibit a strain-hardening phenomenon, effectively recovering nearly all applied deformations at 8% strain. However, loading at 9% and 10% strain results in approximately 1% residual strain. Moreover, there is a notable decrease in phase transformation levels with increased loading amplitude. Interestingly, the reverse transformation levels experience a more pronounced reduction, leading to wider loops at higher loading amplitudes. As depicted in Figure 3(b), stress levels approach nearly 1200 MPa when SMA cables endure a 14% strain load, resulting in a residual strain of 2.4%.

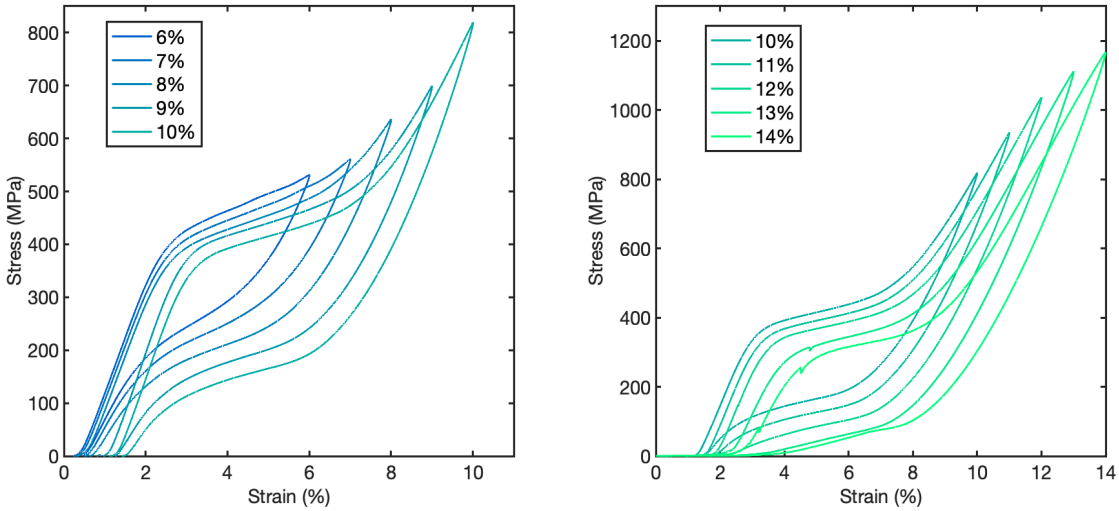

(a) (b)

Figure 3. Stress-strain response of SMAs (a) at 6-10% strain and (b)10-14% strain.

3 Description of Superelastic Friction Damper

Figure 4 presents an exploded view of the Superelastic Friction Damper (SFD). This damper comprises several key components, including SMA cables, inner and outer steel members, friction pads, slotted end plates, and connection plates. The outer member is constructed from a pair of steel channels, featuring friction pads affixed to the exterior face of the web. The inner member consists of I-shaped steel, with the web serving as a sliding interface for the friction pads. An important aspect in achieving enduring, reliable sliding behavior is the careful selection of the friction interface material. In this study friction pads crafted from metal-free brake and clutch lining, often referred to as non-metallic melded strips are used.

By employing brake lining pads in conjunction with stainless steel (BL-SS), self-lubrication of the sliding surface is enabled. This has the positive effect of mitigating the stick-slip phenomenon while maintaining a consistent coefficient of friction, irrespective of the loading rate. Furthermore, this self-lubricating sliding interface exhibits resistance to rust and provides a foundation for long-term, stable performance.

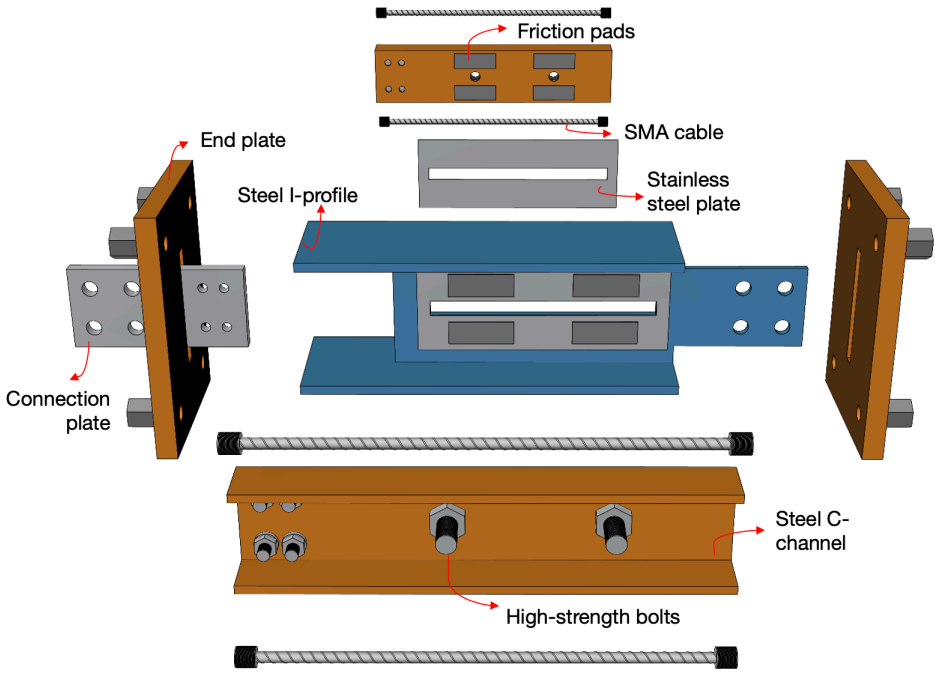

Figure 4. Exploded view of superelastic friction damper (SFD)

4 Experimental response of SFD

A proof-of-concept damper has been designed and fabricated. The geometric details of the specimen are provided in Figure 5. The sizes of the main parts have been determined according to the following basic rules: (i) the strengths of the inner member, outer member, and other accessories are significantly larger than the maximum possible load resistance of the SMA cables plus the frictional force; (ii) the length of the outer and inner members, as well as the distance between the end plates, is dictated by the length of SMA cables, which is determined by the stroke. Both members are composed of low carbon steel (nominal yield strength of 248 MPa). Cyclic loading tests have been conducted to characterize the hysteretic behavior of the SFD. The SFD specimen is connected to an MTS 244 hydraulic actuator, which allows a maximum force of 98 kN and a maximum velocity of 381 mm/sec. The damper force and deformation are measured using the actuator's built-in load cell and LVDT. Two LCWD load cells are used to measure the compression force generated from two friction bolts. The response of the damper at frequencies ranging from 0.02 Hz to 1 Hz is characterized at a displacement amplitude of 20 mm. First, the friction only component of the device is tested and then the complete device is subjected to the same loading protocol. More details about the experimental testing of SFDs can be found in Asfaw et al. (2022).

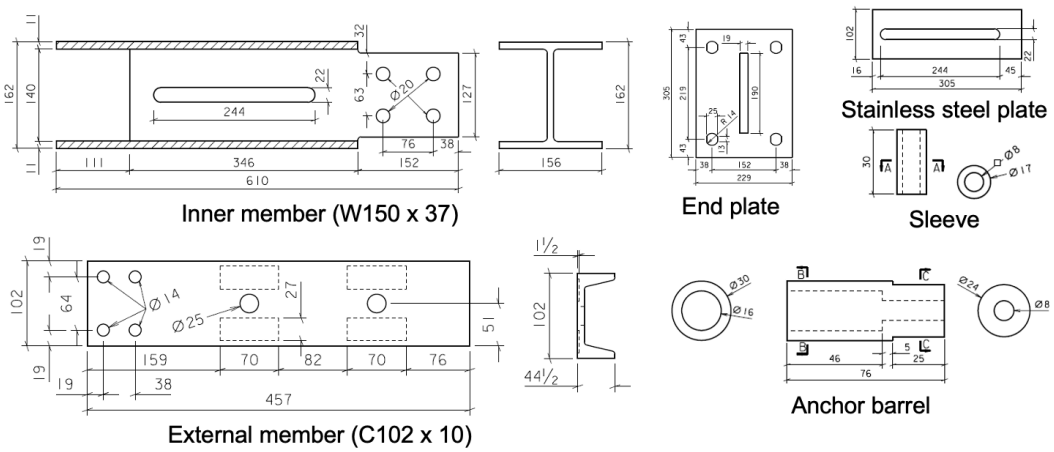

Figure 5. Damper specimen geometric details (unit: mm).

Figure 6 shows the force-displacement response of the damper in the absence of the SMA cables, i.e., frictional component only as well as the complete damper under different loading frequencies. The hysteresis curves are plotted separately for four loading frequencies, namely, 0.02, 0.1, 0.5, and 1 Hz, at a constant amplitude of 20 mm. The overall response of the damper is consistent with the intended working principle. The behaviour of the damper in the two loading directions look symmetrical. In general, the damper displayed a completely stable, repeatable, and reliable behaviour with insignificant dependence on the frequency for the range considered in this study. To better illustrate the effects of loading frequency on the damper response, Figure 7 shows the force-displacement response of the SFD under different loading frequencies on the same plot. As can be seen from Figure 7, there is also no significant effect of loading frequency on the damper response.

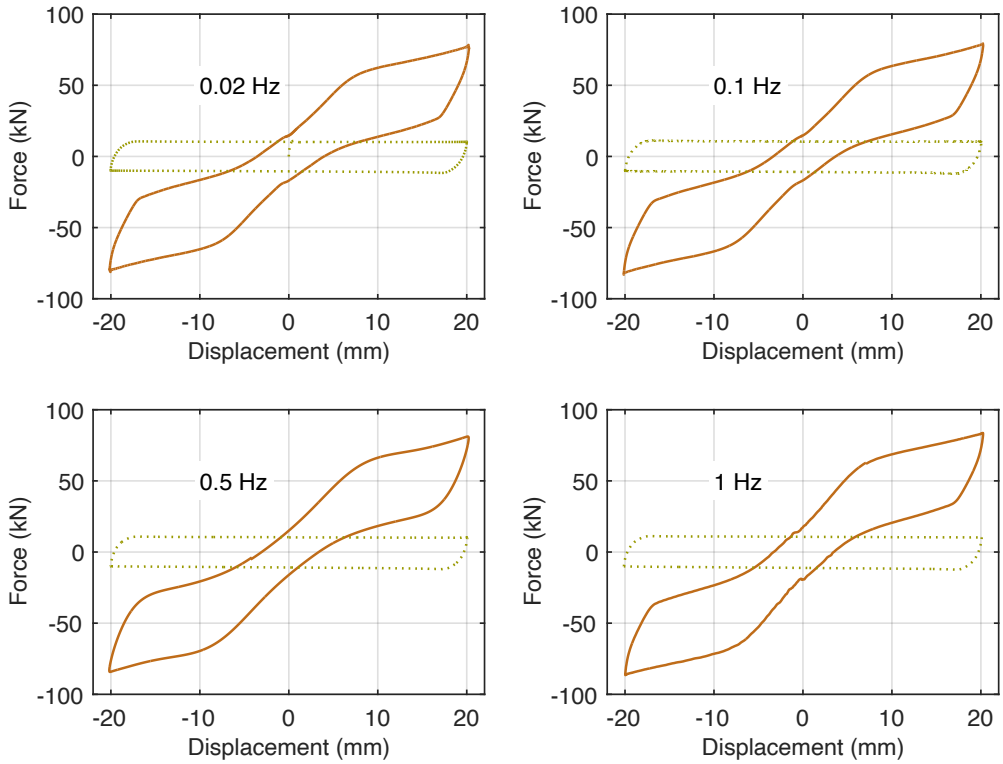

Figure 6. Force-displacement response of the friction only component and complete damper at different loading frequencies.

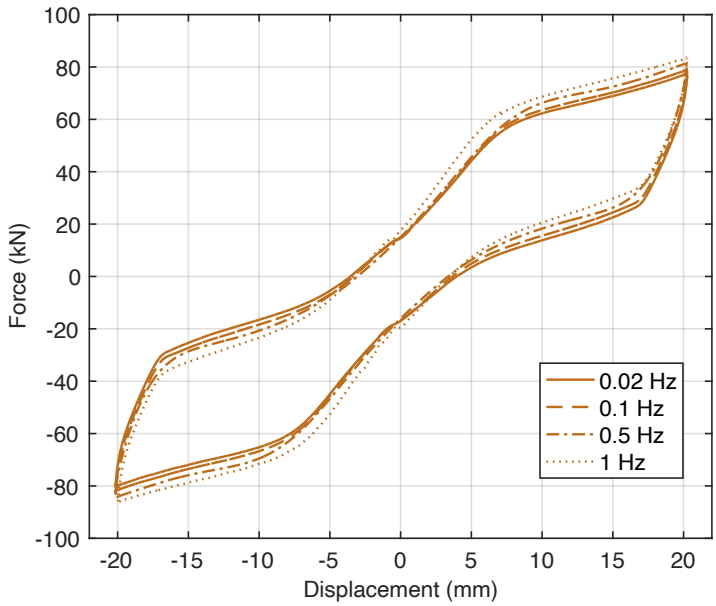

Figure 7. Force-displacement response of SFD at different loading frequencies.

5 Nonlinear Time History Analysis

An 8-story office building, classified as a Risk Category II structure and situated in a Class D soil condition (stiff soil), has been chosen as the subject for numerical investigations. This office building is designed with a dual-system steel frame, incorporating both a lateral force-resisting frame and a gravity frame.The floor framing

layout and the elevation of the specific east-west orientation of this prototype building are depicted in Figure 8. The selected frame is a symmetrical three-span special moment frame (SMF) positioned along the perimeter of the building. The fundamental period of the chosen steel moment-resisting frame is calculated at 3.81 seconds. More comprehensive information regarding the prototype building can be found in Harris and Speicher (2015).

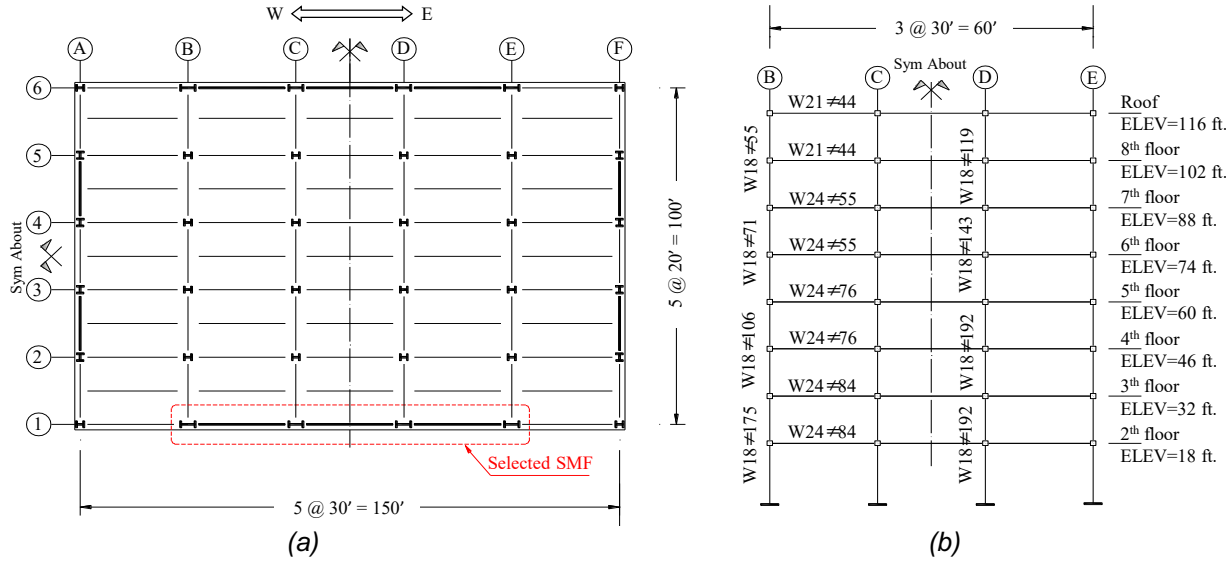

Figure 8. (a) Plan view, and (b) elevation of the archetype building

Numerical modeling of the building is developed in OpenSees. The beam and column components are represented by a concentrated plastic model consisting of elastic beam-column element with rotational springs at both ends to represent plastic hinges. The mechanical behavior of plastic hinges is characterized by using the modified Ibarra–Medina–Krawinkler (IMK) deterioration model for the beams and columns (Ibarra et al. 2005). The shear distortion behavior of the panel zone is modeled following the suggestion of Gupta and Krawinkler and is represented using a trilinear hysteretic model without cyclic degradation considerations (Gupta and Krawinkler 1999). Furthermore, the numerical model accounted for the P-delta effect caused by the interior gravity loads by incorporating an additional leaning column. A Rayleigh damping of 3% is assigned to the steel frame building for numerical modeling. Given that the SFD consists of both SMA and friction components operating in parallel, the mechanical behavior of the SFD is represented in the simulation through the parallel combination of the two distinct mechanical models, namely Steel02 and self-centering.

To evaluate the seismic performance of steel frame using SFD dampers, steel frame is designed using SFD. To this end, the two side spans of the original SMF have been modified to hinged frames with chevron braced damping systems, as shown in Figure 9. Table 1 summaries the mechanical model parameters utilized for various dampers at different floors in each of the three case-study frames. The fundamental periods of the SFD frame is 1.46 s.

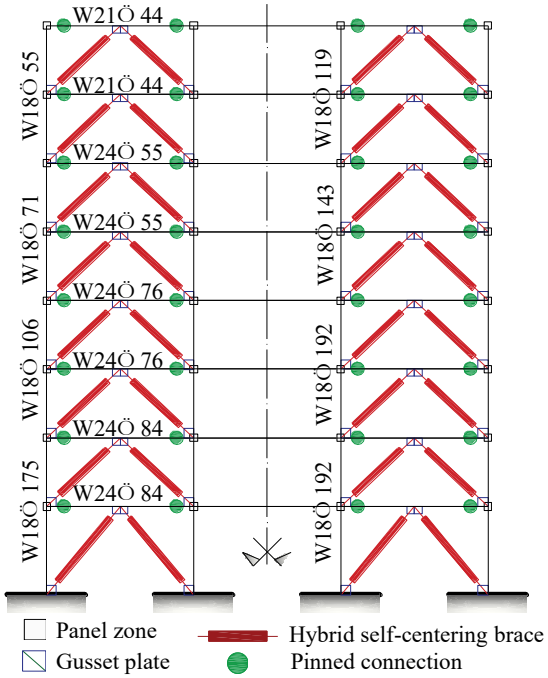

Figure 9. Configuration of steel frame building with SFDs

In order to assess the seismic performance of the steel frame with SFDs, a total of 44 far-filed ground motion records are selected for the nonlinear dynamic analyses. These records are selected from PEER NGA database and recommended by FEMA P695 for structural seismic performance assessment.

The evaluate the seismic response of the SFD frame under design basis earthquake (DBE) and maximum considered earthquake (MCE) hazard levels, all ground motion records are scaled to match with target acceleration spectra at fundamental period of the frame. The nonlinear time history analyses of case-study frame is carried out by using OpenSees. A 10 seconds free vibration time is incorporated after each ground motion record to obtain a relatively stable residual deformation response.

Figure 10 shows the inter-story drift ratio (IDR) response of second story for the case-study frame under Imperial Valley/Delta record at MCE hazard level. The peak response and residual inter-story drift ratio (RIDR) are also highlighted and given in the figure. The IDR for the SFD frame is 2.37% while the residual inter-story drift ratios (RIDR) for the frame is only 0.021%. This indicates that the SFD frame is able to completely eliminate residual drifts even after subjected to an MCE-level earthquake.

The hysteresis responses of the SFD at the second story, subjected to the Imperial Valley/Delta record at the Maximum Considered Earthquake (MCE) hazard level, are depicted in Figure 11. The displacement and force values in the figure represent the ultimate response of the damper following 10 seconds of free vibration. Upon experiencing the earthquake excitation from the Imperial Valley/Delta, the SFD damper exhibits a final residual deformation of merely 1.1 mm. This slight residual deformation of the SFD, at 1.1 mm, underscores its efficacy in controlling structural residual deformation during seismic events.

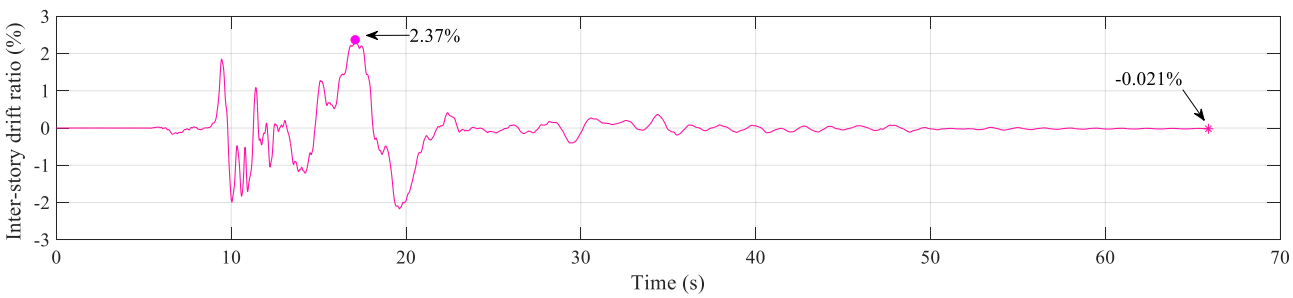

(a)

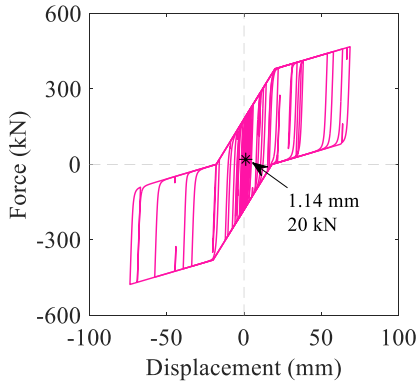

(b)

Figure 10. (a) Time-history response of second story drifts and (b) hysteretic response of SFD under Imperial Valley/Delta record at MCE hazard level.

Figure 11 presents a boxplot that statistically summarizes the maximum seismic response of IDR, RIDR, and AA for the three case-study frames under 44 far-field ground motion records at DEB and MCE hazard levels. The boxplot comprises a central red mark denoting the median (with a specific value also provided), whereas the bottom and top edges of the box represent the 25th and 75th percentiles, respectively. The whiskers extend to the extreme data, excluding outliers, which are illustrated as individual points. It can be observed that the median IDRs of SFD frame under DBE and MCE hazard levels are 1.69% and 2.75%, respectively. The IDR responses under the two hazard levels satisfy the requirements specified in the ASCE 7 due to the installation of the SFD devices, and they are significantly lower than the code limits. As for the RIDR, the median values are 0.06% and 0.08% under the DBE and MCE hazard levels, respectively, which can be considered negligible. According to FEMA P58, if the RIDR is less than 0.2%, no adjustment or strengthening of the structure is required. Regarding the absolute acceleration (AA), as the seismic intensity increases from the DBE to the MCE level, the AA increases by a factor of 1.51. This is because the AA is highly sensitive to the energy dissipation capacity, which is not an advantage of the self-centering device.

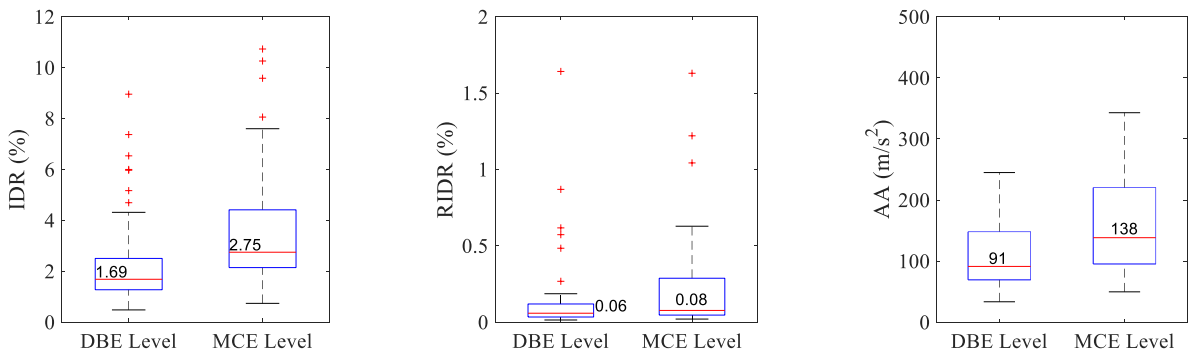

(a) (b) (c)

Fig. 11. Boxplot of (a) IDR, (b) RIDR and (c) AA for SFD frame under DBE and MCE levels.

6 Conclusions

This study introduces the Superelastic Friction Damper (SFD), a novel hybrid damper that combines the advantageous properties of shape memory alloy (SMA) cables and a frictional damping device. Experimental testing demonstrates the excellent mechanical response of SFD in terms of energy dissipation capacity and self-centering ability under repeated cyclic loading at various displacement amplitudes and loading rates. The SFD possesses stable hysteretic behavior with minimal sensitivity to loading rate, providing an equivalent viscous damping of 12% and an impressive recovery capability. Additionally, numerical analysis using OpenSees reveals the positive impact of the SFD on enhancing the seismic performance of a steel frame structure, particularly in reducing the residual inter-story drift ratio (RIDR). The incorporation of the SFD offers promising prospects for improving the seismic performance of steel frame buildings by providing enhanced energy dissipation capacity and self-centering capability.

Overall, the SFD presents a valuable contribution to the field of structural engineering, offering an innovative solution for mitigating seismic hazards in steel frame structures. Further research are warranted to fully explore its potential, validate its effectiveness in enhancing the seismic resilience of buildings, and expediate its application in real-world scenarios.

7 References

Asfaw, A. M., Cao, L., Ozbulut, O. E., & Ricles, J. (2022). Development of a shape memory alloy-based friction damper and its experimental characterization considering rate and temperature effects. Engineering Structures, 273, 115101.

Fang, C., Wang, W., & Shen, D. (2021). Development and experimental study of disc spring–based self-centering devices for seismic resilience. *Journal of Structural Engineering*, 147(7), 04021094.

Issa, A. S., & Alam, M. S. (2019). Experimental and numerical study on the seismic performance of a self-centering bracing system using closed-loop dynamic (CLD) testing. *Engineering Structures*, 195, 144-158.

Li, J., Wang, W., & Cao, Z. (2021). Self-centering hybrid dampers for improving seismic resilience. *Engineering Structures*, 244, 112829.

Ozbulut, O. E., Hurlebaus, S., & DesRoches, R. (2011). Seismic response control using shape memory alloys: a review. *Journal of Intelligent Material Systems and Structures*, 22(14), 1531-1549.

Ramirez, C. M., & Miranda, E. (2012). Significance of residual drifts in building earthquake loss estimation. *Earthquake Engineering & Structural Dynamics*, 41(11), 1477-1493.

Salehi, M., DesRoches, R., Hodgson, D., & Parnell, T. K. (2021). Numerical evaluation of SMA-based multi-ring self-centering damping devices. *Smart Materials and Structures*, 30(10), 105012.

Shi, F., Zhou, Y., Ozbulut, O. E., & Ren, F. (2022). Hysteretic response and failure behavior of an SMA cable-based self-centering brace. *Structural Control and Health Monitoring*, 29(1), e2847.

Shi. F., Lin. Z., Li. Q., et al. (2023) Design, manufacturing, and testing of a hybrid self-centering brace for seismic resilience of buildings. *Earthquake Engineering & Structural dynamics*, 52(5): 1381-1402.

Shi. F., Saygili. G., Ozbulut. O.E. (2018). Probabilistic seismic performance evaluation of SMA-braced steel frames considering SMA brace failure. *Bulletin of Earthquake Engineering*, 16(12): 5937-5962.

Shi. F., Zhou. Y., Ozbulut. O.E., Cao. S. (2021). Development and experimental validation of anchorage systems for shape memory alloy cables. *Engineering Structures*, 228: 111611.

Silwal. B., Michael. R.J., Ozbulut. O.E. (2015). A superelastic viscous damper for enhanced seismic performance of steel moment frames. *Engineering Structures,* 105: 152-64.

Wang, B., Zhu, S., Chen, K., & Huang, J. (2020). Development of superelastic SMA angles as seismic-resistant self-centering devices. *Engineering Structures*, 218, 110836.

Xu, L. H., Fan, X. W., & Li, Z. X. (2016). Development and experimental verification of a pre-pressed spring self-centering energy dissipation brace. *Engineering Structures*, 127, 49-61.

Zhang, Z., Bi, K., Hao, H., Sheng, P., Feng, L., & Xiao, D. (2020). Development of a novel deformation-amplified shape memory alloy-friction damper for mitigating seismic responses of RC frame buildings. *Engineering Structures*, 216, 110751.